CHAPTER 9

IN-VIVO BIODISTRIBUTION STUDIES

9 IN-VIVO BIODISTRIBUTION STUDIES

9.1 Methods

9.1.1 Animals

All animal experiments conducted were approved by the Social Justice and Empowerment Committee for the purpose of control and supervision on animals and experiments, Ministry of Government of India. Balb/C mice weighing between 25-30gm were selected for biodistribution studies.

9.1.2 Biodistribution and Pharmacokinetic Studies of ETP formulations

Three mice were used at each time point for each formulation. The mice were divided into four groups. Group1 received ^{99m}Tc-ETPS, group2 received ^{99m}Tc-PLGA-ETP-NP and group 3 received ^{99m}Tc-Tf-PLGA-ETP-NP intravenously. Group 4 received ^{99m}Tc-PLGA-ETP-NP administered intranasally. Groups 1 to 3 received 20μCi of radioactivity administered intravenously (100μl) via tail vein. Group 4 received 20μCi of radioactivity administered intranasally (10μl). The mice were sacrificed at different time intervals of 0.5hrs, 1hr, 2 hr, 4hr, 24hrs and blood was collected via cardiac puncture. Different organs including blood, heart, liver, lung, spleen, kidney, brain and stomach were dissected, washed twice with normal saline, made free from any adhering tissues and weighed. The radioactivity present in each tissue/organ was determined using shielded well-type gamma scintillation counter along with 3 samples of standard solution representing 100% of the administered dose. The radioactivity in each tissue/organ was determined as fraction of administered dose per gram of the tissue (%A/g). The results of radioactivity measured at various time points in different organs are recorded in Table 9.1,9.2, 9.3 and 9.4 for ^{99m}Tc-ETPS, ^{99m}Tc-PLGA-ETP-NP (IV), ^{99m}Tc-Tf-PLGA-ETP-NP and ^{99m}Tc-PLGA-ETP-NP (IN) respectively.. The blood concentrations vs. time (hrs) are plotted in Figure 9.1. Figure 9.2 represents the brain concentrations vs. time profile.

Statistical Analysis

All data are reported as mean ± SD (standard deviation) and the difference between the groups were tested using Student's t-test at the level of $P<0.05$. Pharmacokinetic

parameters were calculated using Kinetica (version 4.40, Innaphase, Philadelphia, PA, USA) applying non compartmental kinetics for IV bolus. The pharmacokinetic parameters are recorded in Table 9.5. The AUC for the brain are recorded in Table 9.6. Statistical evaluation was compared using ANOVA and differences greater at $p<0.05$ were considered significant.

Gamma Scintigraphy Studies

Gamma Scintigraphy was done in mice after administering 100µl of ^{99m}Tc-labeled complexes of ETPS, PLGA-ETP-NPs and Tf-PLGA-ETP-NPs containing 100µCi of 99mTc was intravenously injected. The animals were anaesthetized using chloroform and mount on a wooden board. The imaging was performed on single photon emission computerized tomography (SPECT, LC 75-005, Diacam, Siemens, Hoffman Estates, IL, USA) after 2 hrs. The gamma scintigraphic image is shown in figure 9.3

9.1.3 Biodistribution and Pharmacokinetic studies of TMZ formulations

The biodistribution studies for Temozolomide and its nanoparticles were conducted in the same way and protocol as that of etoposide and its nanoparticles. The results of radioactivity at different time points in different organs are recorded in Table 9.7, 9.8, 9.9 and 9.10 for ^{99m}Tc-TMZS, ^{99m}Tc-PLGA-TMZ-NP (IV), ^{99m}Tc-Tf-PLGA-TMZ-NP and ^{99m}Tc-PLGA-TMZ-NP (IN). The blood concentrations vs. time (hrs) are plotted in Figure 9.4. Figure 9.5 represents the brain concentrations vs. time profile. The pharmacokinetic parameters are recorded in Table 9.11. The AUC for the brain are recorded in Table 9.12. Statistical evaluation was compared using ANOVA and differences greater at $p<0.05$ were considered significant. The gamma scintigraphic image is shown in figure 9.6

9.2 Result and Discussion

9.2.1 Biodistribution and Pharmacokinetic Studies of ETP formulations

The radiolabeled complexes of ETPS, PLGA-ETP-NP and Tf-PLGA-ETP-NP were evaluated for biodistribution in balb/c mice for 24 hrs after intravenous injection and PLGA-ETP-NP intranasal administration as well. The results of biodistribution for various radiolabelled complexed formulations are tabulated in table 9.1, 9.2, 9.3, and 9.4. The results of biodistribution studies reveal that ETPS blood circulation time gets significantly enhanced after its incorporation in PLGA nanoparticles.

Table 9.1: Biodistribution of ^{99m}TC labelled ETPS

Organ/Tissue	%A/g (Mean ± SD)				
	0.5hr	1hr	2hr	4hr	24hr
Blood	3.41 ± 0.29	2.62 ± 0.17	2.0 ± 0.24	1.09 ± 0.08	0.28 ± 0.06
Brain	0.08 ± 0.02	0.06 ± 0.02	0.04 ± 0.02	0.03 ± 0.01	0.01 ± 0.01
Liver	50.68 ± 2.42	41.05 ± 1.23	33.97 ±1.98	25.61 ± 1.06	3.13 ± 0.86
Lung	0.24 ± 0.04	0.20 ± 0.01	0.18 ± 0.02	0.13 ± 0.04	0.072 ± 0.02
Kidney	13.03 ± 1.29	10.42 ± 1.08	8.92 ± 0.73	5.54 ± 0.43	1.51 ± 0.14
Spleen	4.94 ± 0.15	5.89 ± 0.21	6.76 ± 0.42	6.05 ± 0.36	2.3 ± 0.19
Heart	1.92 ± 0.08	2.32 ± 0.05	1.74 ± 0.01	0.97 ± 0.02	0.39 ± 0.03
Stomach	0.03 ± 0.01	0.06 ± 0.02	0.08 ± 0.02	0.05 ± 0.03	0.04 ± 0.01

Results expressed as percentage activity of injected dose per gram of tissue. Each value is expressed as mean of three separate determinations (n=3)

Table 9.2: Biodistribution of ^{99m}TC labelled PLGA-ETP-NP (IV)

Organ/Tissue	%A/g (Mean ± SD)				
	0.5hr	1hr	2hr	4hr	24hr
Blood	5.15 ± 0.52	3.78 ± 0.24	3.05 ± 0.38	2.35 ± 0.19	1.24 ± 0.12
Brain	0.1 ± 0.02	0.13 ± 0.01	0.09 ± 0.01	0.07 ± 0.03	0.03 ± 0.02
Liver	39.4 ± 2.83	35.09 ± 1.49	28.58 ± 0.84	14.82±1.08	6.86 ± 0.41
Lung	2.33 ± 0.11	2.57 ± 0.14	2.49 ± 0.17	2.01 ± 0.09	0.82 ± 0.07
Kidney	5.21 ± 0.13	6.29 ± 0.08	6.72 ± 0.07	5.48 ± 0.21	3.7 ± 0.14
Spleen	7.37 ± 0.17	8.2 ± 0.69	8.68 ± 0.44	7.15 ± 0.18	2.14 ± 0.11
Heart	1.02 ± 0.08	0.94 ± 0.07	0.81 ± 0.11	0.72 ± 0.16	0.13 ± 0.05
Stomach	0.11 ± 0.04	0.04 ± 0.02	0.16 ± 0.04	0.21 ± 0.05	0.43 ± 0.03

Results expressed as percentage activity of injected dose per gram of tissue. Each value is expressed as mean of three separate determinations (n=3)

Table 9.3 : Biodistribution of ^{99m}TC labelled Tf-PLGA-ETP-NP

Organ/Tissue	%A/g (Mean ± SD)				
	0.5hr	**1hr**	**2hr**	**4hr**	**24hr**
Blood	5.50 ± 0.48	4.51 ± 0.32	3.79 ± 0.29	3.28 ± 0.10	1.82 ± 0.37
Brain	0.17 ± 0.05	0.32 ±0.04	0.43 ± 0.08	0.37 ± 0.04	0.14 ± 0.02
Liver	24.61 ± 3.82	26.88 ±2.14	20.45 ± 2.78	12.24 ± 1.49	5.62 ± 1.21
Lung	1.93 ± 0.23	2.78 ± 0.31	2.21 ± 0.23	1.78 ± 0.15	0.65 ± 0.25
Kidney	4.71 ± 0.29	5.43 ± 0.17	6.91 ± 0.38	5.82 ± 0.17	4.45 ± 0.11
Spleen	6.76 ± 0.49	7.43 ± 0.29	10.18 ± 0.72	8.1 ± 0.11	3.95 ± 0.18
Heart	0.91 ± 0.05	0.89 ± 0.11	0.84 ± 0.14	0.62 ± 0.10	0.19 ± 0.02
Stomach	0.12 ± 0.03	0.34 ± 0.01	0.38 ± 0.03	0.45 ± 0.02	0.89 ± 0.04

Results expressed as percentage activity of injected dose per gram of tissue. Each value is expressed as mean of three separate determinations (n=3)

Table 9.4: Biodistribution of ^{99m}TC labelled PLGA-ETP-NP (IN)

Organ/Tissue	%A/g (Mean ± SD)				
	0.5hr	**1hr**	**2hr**	**4hr**	**24hr**
Blood	0.74 ± 0.21	1.35 ± 0.16	1.06 ± 0.07	0.90 ± 0.13	0.22 ± 0.12
Brain	0.14 ± 0.10	0.24 ± 0.08	0.17 ± 0.04	0.13 ± 0.04	0.07 ± 0.05
Liver	1.18 ± 0.14	1.44 ± 0.11	1.01 ± 0.23	0.91 ± 0.07	0.59 ± 0.06
Lung	1.07 ± 0.07	1.22 ± 0.33	1.15 ± 0.14	0.99 ± 0.11	0.18 ± 0.03
Kidney	1.41 ± 0.13	2.45 ± 0.21	2.29 ± 0.29	2.19 ± 0.17	0.92 ± 0.12
Spleen	1.62 ± 0.17	2.57 ± 0.21	3.01 ± 0.18	3.12 ± 0.24	1.32 ± 0.15
Heart	0.48 ± 0.04	0.41 ± 0.07	0.92 ± 0.06	0.32 ± 0.04	0.11 ± 0.03
Stomach	13.92 ± 2.73	14.5 ± 1.91	15.86 ± 2.31	16.64 ± 1.17	15.98 ± 0.68

Results expressed as percentage activity of injected dose per gram of tissue. Each value is expressed as mean of three separate determinations (n=3)

Figure 9.1: Blood concentration Vs. Time (hr) plot for ^{99m}TC - Etoposide formulations

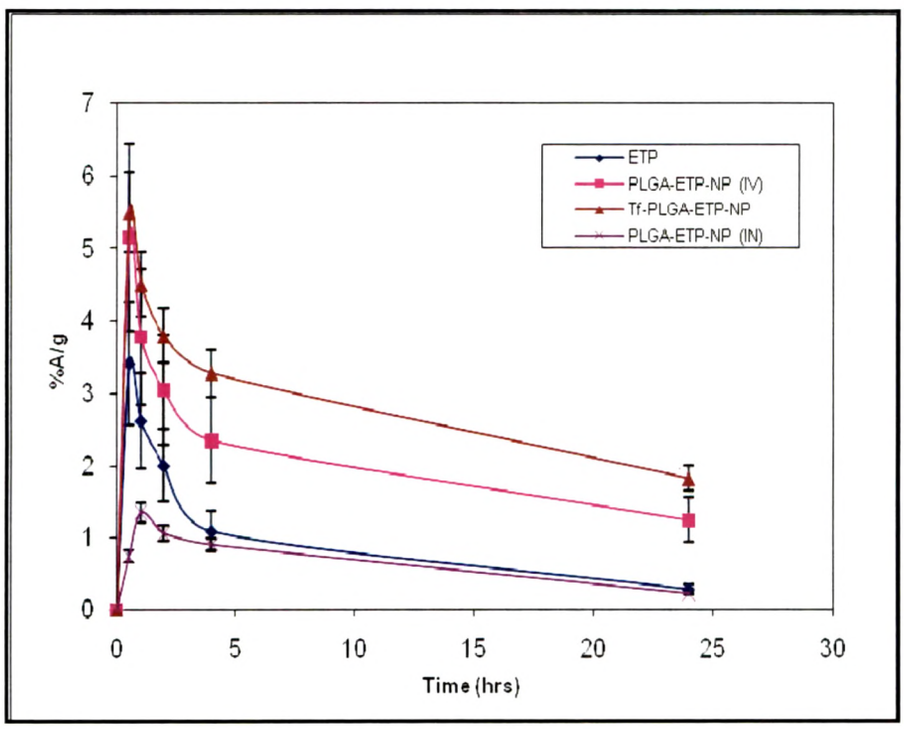

Blood concentrations vs. time plot of the different radiolabelled formulations are shown in figure 9.1. The results of the studies depict faster elimination of ETPS from the body. Lower blood ETP concentration was found in the blood with 3.41 %A/g at 0.5hrs of ETPS compared to 5.15% A/g and 5.50 %A/g for PLGA-ETP-NP and Tf- PLGA-ETP-NP after intravenous injection respectively. At 24 hrs, the blood concentration of Tf conjugated nanoparticles and unconjugated nanoparticles was found to be 1.82%A/g and 1.34%A/g respectively, which is 6.5 times and 4.78 times higher than etoposide solution exhibiting 0.28%A/g. These findings are indicative of the increased residence time and slower elimination of drug loaded nanoparticles. This increase in the residence time may be attributed to slow opsonisation from blood caused by smaller size of nanoparticle (≤200nm) of nanoparticles [Moghimi et al., 1993] and presence of hydrophilic PVA on the nanoparticles surface providing hydrophilic covering around the particles [Sahoo et al., 2002]. The blood concentration after intranasal administration of PLGA-ETP-NP was found to be less than the intravenously administered drug solution and the nanoparticle formulations.

The pharmacokinetic parameters of etoposide in mice after intravenous administration of drug solution and drug loaded nanoparticles including intranasal administration of unconjugated drug nanoparticles have been recorded in Table 9.5.

Table 9.5: Pharmacokinetic parameters of Etoposide formulations

Pharmacokinetic Parameter	ETPS	PLGA-ETP-NP (IV)	TF- PLGA-ETP-NP	PLGA-ETP-NP (IN)
T_{max} (hr)	0.5	0.5	0.5	1
C_{max} (%A/g)	3.41	5.15	5.50	1.35
$AUC_{(0\rightarrow\infty)}$ (hr)*(%A/g)	23.98	81.51**	123.43*	16.88
$T_{1/2}$ (hrs)	8.59	18.59**	21.82*	9.75
MRT(hrs)	11.70	28.53	31.22	14.16

*P<0.05, Significantly higher than to other groups

** P<0.05, Significantly higher than ETPS and PLGA-ETP-NP (IN)

Significant differences (P<0.05) in results of various pharmacokinetic parameters were observed after iv administration of ETPS and Tf-PLGA-ETP-NP. The plasma $AUC_{(0\rightarrow\infty)}$, MRT and $T_{1/2}$ of TF-PLGA-ETP-NP were found to be significantly higher than etoposide solution. For TF-PLGA-ETP-NP, the $AUC_{(0\rightarrow\infty)}$, MRT and $T_{1/2}$ observed were respectively 5.15, 2.67 and 2.44 folds higher than ETPS. The unconjugated nanoparticles administered intravenously demonstrated significantly higher $AUC_{(0\rightarrow\infty)}$, MRT and $T_{1/2}$ than drug solution and intranasally administered unconjugated nanoparticles. The high values of MRT and $T_{1/2}$ for PLGA-ETP-NP and TF-PLGA-ETP-NP are indicative of slow clearance and long blood circulation of drug nanoparticles.

The major amount of the injected dose was found to accumulate in the organs of reticuloendothelial system comprising liver and spleen. The distribution results show high accumulation of ETPS than PLGA-ETP-NP and Tf-PLGA-ETP-NP in liver. At 0.5hrs after injection, ETPS shows 50.68%A/g as compared to 39.40%A/g and 24.61%A/g for PLGA-ETP-NP and Tf-PLGA-ETP-NP respectively. The low accumulation of nanoparticles may be due to the hydrophilicity associated with the nanoparticle surface, as mentioned earlier. Further, transferrin as reported could have masked the recognization sites on the colloidal systems thereby reducing the liver uptake [Litzinger et al., 1994; V. Soni et al., 2008]. The overall uptake of nanoparticles in

comparison to etoposide solution increased in the spleen after intravenous administration. As depicted in results, the uptake of PLGA-ETP-NP and Tf-PLGA-ETP-NP in the spleen is found to be 8.68%A/g and 10.18A%/g at 2hrs, while ETPS showed 6.76%A/g at the same time. The retention of nanoparticles in the reticular fibre meshwork and the macrophages in red pulp of spleen may be attributed to this high accumulation (Litzinger et al. 1994). These results indicate the major role of liver and spleen in the clearance of drug in solution and nanoparticle formulations.

The distribution results in the kidney indicate higher values for ETPS then PLGA-ETP-NP and Tf- PLGA-ETP-NP. At 0.5hrs after intravenous injection, ETPS shows higher accumulation in kidney at 13.03%A/g with respect to 5.21%A/g for PLGA-ETP-NP and 4.71%A/g for Tf- PLGA-ETP-NP, indicating fast clearance of etoposide solution than the nanoparticle formulation. The radioactivity at 24hrs is lower for ETPS (1.51%A/g) as that of PLGA-ETP-NP (3.7%A/g) and Tf- PLGA-ETP-NP (4.45%A/g), confirming the higher elimination half life for drug encapsulated PLGA nanoparticles.

The radioactivity measured indicates higher accumulation of unconjugated and conjugated nanoparticles than plain etoposide in the lungs. This enhanced deposition is resulted due to the size of the nanoparticles. The values of radioactivity for distribution to heart indicate significantly higher values for etoposide solution than the nanoparticle formulation at all time points. This indicates potential reduction in cardiotoxicity associated with etoposide using the nanoparticle formulation.

The brain is the main organ of investigation in the present study. Figure 9.2 shows the brain distribution curve of ETPS, PLGA-ETP-NP (IV), Tf-PLGA-ETP-NP and PLGA-ETP-NP (IN).

Figure 9.2: Brain concentration Vs. Time (hr) plot for ^{99m}TC - Etoposide formulations

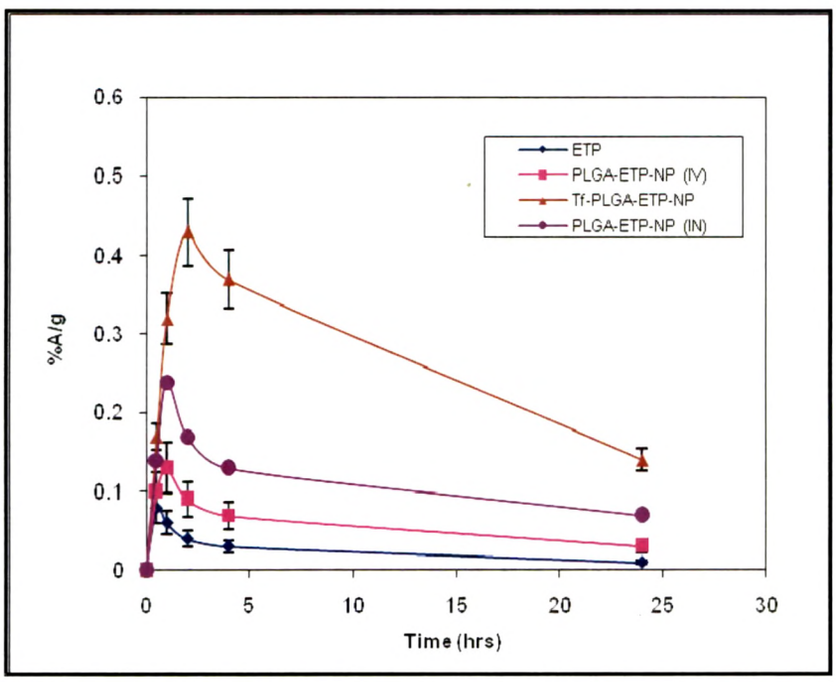

It is evident from results that the brain uptake of etoposide was lower than the nanoparticle formulations. The peak concentration for ETPS in brain was found to be 0.08%A/g at 0.5hrs after intravenous injection. At 24hrs, the concentration of ETPS in brain recorded was very low with 0.01 %A/g. The distribution of nanoparticle formulations demonstrate enhanced deposition in the brain. The peak concentrations for PLGA-ETP-NP and Tf-PLGA-ETP-NP were found to be 0.13%A/g and 0.43%A/g attained at 1hr and 2hrs respectively after intravenous administration. At 24hrs after intravenous injection the unconjugated nanoparticles show 3 folds increase in brain concentration i.e. 0.03%A/g, as that of ETPS. Tf conjugated nanoparticles with 0.14%A/g at 24hrs, exhibit 14 folds and 4.66 folds higher uptake in brain than plain drug and unconjugated nanoparticles respectively. Also, the radioactivity observed after 24hrs for Tf-PLGA-ETP was even higher than the peak concentration of ETPS.

The intranasal administration of PLGA-ETP-NP led to significantly superior brain deposition than the intravenous injection of same formulation and ETPS. The brain concentrations at 0.5hr and 1hr post intranasal administration of PLGA-ETP-NP were found to be 0.14%A/g and 0.24%A/g respectively. At 24hrs, the brain concentrations were more than twice that of the same formulation administered intravenously. However, overall brain accumulation after intranasal administration of PLGA-ETP-NP was significantly lower when compared with intravenous injection of Tf-PLGA-ETP-NP.

Table 9.6: AUC values of brain for Etoposide formulations

Parameter/ Formulation	ETPS	PLGA-ETP-NP (IV)	Tf-PLGA-ETP-NP	PLGA-ETP-NP (IN)
AUC (0→24)	0.5377	1.2946***	6.0716*	2.5696**
AUC (0→∞)	0.7051	1.9347***	8.8701*	4.4859**

* P<0.05, Significantly higher than Tf-PLGA-ETP-NP as compared to other groups
** P<0.05, Significantly higher than PLGA-ETP-NP(IN) as compared to ETPS and PLGA-ETP-NP (IV) groups
***P<0.05, Significantly higher than ETPS

The overall brain uptake demonstrated by AUC $_{(0\rightarrow24)}$ brain for different groups is tabulated in table 9.6. The AUC $_{(0\rightarrow24)}$ brain for Tf-PLGA-ETP-NP was calculated to be 11.29 folds and 4.69 folds significantly higher than ETPS and PLGA-ETP-NP after intravenous administration. When compared with intranasal administration of PLGA-ETP-NP, AUC $_{(0\rightarrow24)}$ brain for Tf-PLGA-ETP-NP was 2.36 folds higher. However, PLGA-ETP-NP after intranasal administration exhibits significantly higher brain AUC $_{(0\rightarrow24)}$ at 1.98 folds and 4.77 folds compared to PLGA-ETP-NP and ETPS administered intravenously.

Poor brain uptake of ETPS is due to its inability to permeate across the BBB and it being substrate to Pgp (MDR1), efflux transporters, present at the blood brain barrier. The unconjugated and Tf conjugated nanoparticles show improved brain uptake of drug. The hydrophilic surface characteristic of the nanoparticles, due to the surface crosslinked PVA, could have led to increase in the residence time in blood and thereby leading to enhanced brain deposition. The preferential accumulation of Tf-PLGA-ETP-NP across the BBB may be the result of different events. The abundance of transferrin receptors on BBB could have resulted in the receptor mediated endocytosis, thereby transporting the

particulates to the brain. [Pardridge et al., 1987; Roberts et al., 1993; Mishra et al., 2006; Soni et al., 2008] Further, it is also reported that transferrin-drug conjugate leads to the invitro inhibition of multi drug resistance protein highly expressed on resistant cancer cells. This event could have resulted in inhibition of multi drug resistance protein expressed on BBB, thereby preventing efflux of Tf-PLGA-ETP-NP [Sahoo and Labhasetwar, 2005]. Also, the actual condition of brain tumors leads to disruption of BBB, which may further enhance the better accumulation of the delivery system [Ningaraj, 2006]. The intranasal administration of PLGA-ETP-NP increased brain concentrations as compared to the intravenous administration of same formulation and ETPS. The radioactivity detected in blood circulation after intranasal administration of PLGA-ETP-NP was significantly lower ($P<0.05$) than the same formulation administered intravenously. This indicates the direct transport of the nanoparticles to the brain through the olfactory route bypassing the blood brain barrier. [Illum, 2000]

Gamma Scintigraphy Studies

To ascertain the brain targeting following intravenous administration of ^{99m}Tc etoposide loaded nanoparticles, gamma scintigraphy was performed and scintigrams after 2 hrs post intravenous injection are shown in Figure 9.3.

Figure 9.3: Gamma Scintigraphy image of mice after 2hrs of intravenous injection of ETPS (A), PLGA-ETP-NP (B) and Tf-PLGA-ETP-NP (C)

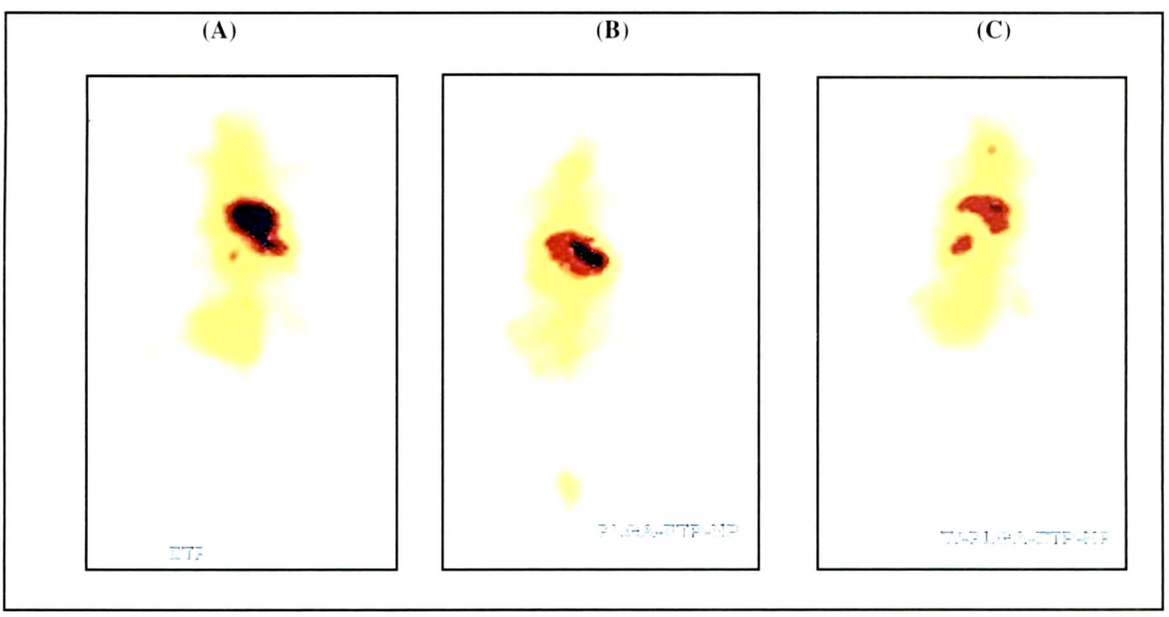

The major radioactivity deposition is seen in liver and spleen, in confirmation to the biodistribution studies. The brain deposition shows higher accumulation of Tf-PLGA-ETP-NP in brain, following intravenous administration, as compared to PLGA-ETP-NP and ETPS is clearly depicted in the scintigram.

9.2.2 Biodistribution and Pharmacokinetic Studies of TMZ formulations

Similarly for tmozolomide, the results of biodistribution for various radiolabeled complexed formulations are tabulated in table 9.7, 9.8, 9.9, and 9.10. The results of biodistribution studies reveal that TMZS blood circulation time gets significantly enhanced after its incorporation in PLGA nanoparticles.

Table 9.7: Biodistribution of ^{99m}Tc labeled TMZS

Organ/Tissue	%A/g (Mean ± SD)				
	0.5hrs	1 hr	2hrs	4hr	24hr
Blood	2.89 ± 0.48	2.16 ± 0.26	1.62 ± 0.12	0.91 ± 0.06	ND
Brain	0.14 ± 0.02	0.11 ± 0.02	0.08± 0.03	0.05 ± 0.01	0.01 ± 0.002
Liver	60.65 ± 3.97	55.18 ± 4.12	43.29 ± 2.69	32.61 ± 2.26	4.89 ± 0.44
Lung	0.32 ± 0.07	0.26 ± 0.04	0.24 ± 0.07	0.17 ± 0.02	0.1 ± 0.01
Kidney	16.29 ± 1.48	12.68 ± 1.17	8.59 ± 0.61	4.98 ± 0.29	0.69 ± 0.04
Spleen	13.33 ± 0.97	11.34 ± 1.02	8.76± 0.89	7.16 ± 0.36	1.79 ± 0.09
Heart	1.46 ± 0.11	2.59 ± 0.26	2.18 ± 0.14	1.63 ± 0.11	0.59 ± 0.09
Stomach	0.02 ± 0.01	0.05 ± 0.02	0.08 ± 0.02	0.12 ± 0.04	0.09 ± 0.03

Results expressed as percentage activity of injected dose per gram of tissue. Each value is expressed as mean of three separate determinations (n=3)

Table 9.8: Biodistribution of ^{99m}Tc labeled PLGA-TMZ-NP (IV)

Organ/Tissue	%A/g (Mean ± SD)				
	0.5hrs	1 hr	2hrs	4hr	24hr
Blood	4.53 ± 0.36	2.95 ± 0.16	2.5 ± 0.14	1.89 ± 0.13	0.83 ± 0.1
Brain	0.11 ± 0.02	0.17 ± 0.02	0.12 ± 0.01	0.08 ± 0.01	0.04 ± 0.002
Liver	44.92 ± 3.29	35.79 ± 2.11	29.15 ± 2.26	20.68 ± 1.88	6.27 ± 0.43
Lung	2.63 ± 0.19	2.9 ± 0.21	2.81 ± 0.17	2.27 ± 0.19	0.93 ± 0.16
Kidney	6.51 ± 0.53	7.55 ± 0.46	8.87 ± 0.36	6.52 ± 0.41	2.23 ± 0.18
Spleen	8.11 ± 0.6	9.02 ± 0.11	10.42 ± 0.92	7.51 ± 0.32	2.65 ± 0.21
Heart	0.86 ± 0.12	1.04 ± 0.08	1.29 ± 0.11	0.92 ± 0.11	0.39 ± 0.06
Stomach	0.18 ± 0.01	0.21 ± 0.03	0.26 ± 0.03	0.68 ± 0.05	0.87 ± 0.09

Results expressed as percentage activity of injected dose per gram of tissue. Each value is expressed as mean of three separate determinations (n=3)

Table 9.9: Biodistribution of ^{99m}Tc labeled Tf-PLGA-TMZ-NP

Organ/Tissue	%A/g (Mean ± SD)				
	0.5hrs	1 hr	2hrs	4hr	24hr
Blood	5.18 ±0.46	3.68 ± 0.22	2.98 ± 0.26	2.36 ± 0.15	1.19 ± 0.13
Brain	0.21 ± 0.03	0.36 ± 0.04	0.44 ± 0.07	0.39 ± 0.02	0.19 ± 0.03
Liver	28.39 ±2.18	34.26 ± 1.86	28.62 ± 3.02	22.57 ± 2.06	6.57 ± 0.31
Lung	1.12 ± 0.14	1.28 ± 0.07	1.46 ± 0.1	1.04 ± 0.07	0.19 ± 0.04
Kidney	5.08 ± 0.32	6.42 ± 0.36	7.57 ± 0.59	4.96 ± 0.19	2.41 ± 0.16
Spleen	8.25 ± 0.61	9.81 ± 0.78	12.01 ± 1.34	9.32 ± 0.47	3.41 ± 0.23
Heart	0.62 ±0.41	0.79 ± 0.09	0.92 ± 0.11	0.52 ± 0.03	0.32 ± 0.02
Stomach	0.32 ± 0.06	0.42 ± 0.05	0.46 ± 0.05	0.53 ± 0.05	0.92 ± 0.08

Results expressed as percentage activity of injected dose per gram of tissue. Each value is expressed as mean of three separate determinations (n=3)

Table 9.10: Biodistribution of ^{99m}Tc labeled PLGA-TMZ-NP (IN)

Organ/Tissue	%A/g (Mean ± SD)				
	0.5hrs	1 hr	2hrs	4hr	24hr
Blood	0.91 ± 0.07	1.29 ± 0.16	0.98 ± 0.12	0.78 ± 0.1	0.12 ± 0.01
Brain	0.17 ± 0.01	0.31 ± 0.03	0.22 ± 0.01	0.14 ± 0.02	0.07 ± 0.003
Liver	1.22 ± 0.16	1.5 ± 0.17	1.34 ± 0.09	1.12 ± 0.18	0.76 ± 0.13
Lung	2.08 ± 0.23	3 ± 0.34	2.39 ± 0.18	1.92 ± 0.1	0.7 ± 0.08
Kidney	2.41 ± 0.19	2.89 ± 0.18	3.11 ± 0.24	3.36 ± 0.41	1.01 ± 0.11
Spleen	1.76 ± 0.11	2.17 ± 0.2	2.89 ± 0.31	3.78 ± 0.28	1.29 ± 0.09
Heart	0.29 ± 0.02	0.47 ± 0.05	0.52 ± 0.07	0.74 ± 0.03	0.46 ± 0.03
Stomach	14.78 ± 1.98	15.93 ± 1.37	16.43 ± 1.44	16.78 ± 2.1	15.23 ± 1.16

Results expressed as percentage activity of injected dose per gram of tissue. Each value is expressed as mean of three separate determinations (n=3)

Figure 9.4: Blood concentration Vs. Time (hr) plot for ^{99m}Tc Temozolomide formulations

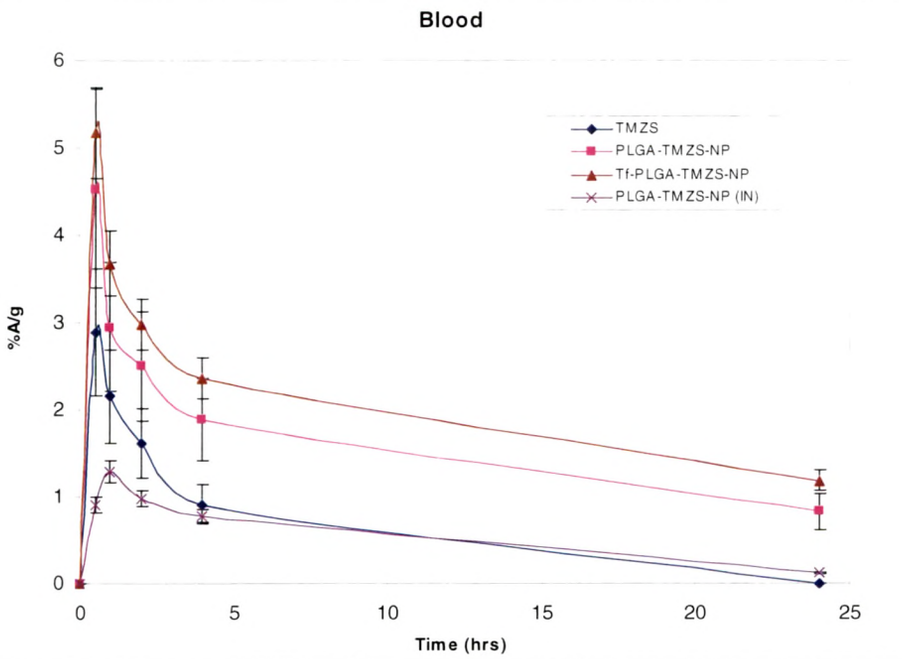

Blood concentrations vs. time plot of the different radiolabeled formulations are shown in figure 9.4. Lower blood TMZS concentration were found in the blood with 2.89 %A/g at 0.5hrs of TMZS compared to 4.53% A/g and 5.18 %A/g for PLGA-TMZ-NP and Tf-PLGA-TMZ-NP after intravenous injection respectively. At 24 hrs, the blood concentration of Tf conjugated nanoparticles and unconjugated nanoparticles were found to be 1.19%A/g and 0.83%A/g respectively. After 24 hrs, no radioactivity was observed in animal group administered with TMZS solution indicating rapid removal of temozolomide in solution form than the nanoparticle formulation. These findings are indicative of the increased residence time and slower elimination of drug from the nanoparticles. The increase in the residence time of the nanoparticles may be attributed to the smaller size of nanoparticle (≤200nm) of nanoparticles [Moghimi et al., 1993] and hydrophilic surface imparted by the presence of the surface crosslinked PVA [Sahoo et al., 2002]. Similar to Etoposide nanoparticles, the intranasal administration of the unconjugated nanoparticles of temozolomide resulted in lower blood concentration than the intravenously administered nanoparticles.

The pharmacokinetic parameters of temozolomide in mice after intravenous administration of drug solution and drug loaded nanoparticles including intranasal administration of unconjugated drug nanoparticles have been recorded in Table 9.11.

Table 9.11: Pharmacokinetic parameters of Temozolomide formulations

Pharmacokinetic Parameter	TMZS	PLGA-TMZ-NP (IV)	TF- PLGA-TMZ-NP	PLGA-TMZ-NP (IN)
T_{max} (hr)	0.5	0.5	0.5	1
C_{max} (%A/g)	2.89	4.53	5.15	1.13
$AUC_{(0\rightarrow\infty)}$ (hr)*(%A/g)	10.2601	54.4699**	78.2941*	12.2647
$T_{1/2}$ (hrs)	2.40	14.91**	17.91*	7.32
MRT(hrs)	3.39	21.24	25.49	10.52

*P<0.05, Significantly higher than to other groups

** P<0.05, Significantly higher than TMZS and PLGA-TMZ-NP (IN)

Significant differences (P<0.05) among results of various pharmacokinetic parameters were observed after intravenous administration of TMZS and Tf-PLGA-TMZ-NP. The plasma AUC $_{(0\rightarrow\infty)}$, MRT and $T_{1/2}$ of TF-PLGA-TMZ-NP were found to be significantly higher than temozolomide solution and unconjugated nanoparticles. For TF-PLGA-TMZ-NP, the AUC $_{(0\rightarrow\infty)}$, MRT observed were respectively 7.63, 7.45 folds higher than TMZS; and 1.44, 1.20 folds higher than the unconjugated nanoparticles. The $T_{1/2}$ for TMZ was observed to be 2.40 hrs as compared to 14.91 and 17.91 hrs for unconjugated and conjugated nanoparticles respectively. The unconjugated nanoparticles administered intravenously demonstrated significantly higher AUC $_{(0\rightarrow\infty)}$, MRT and $T_{1/2}$ than drug solution and intranasally administered unconjugated nanoparticles. The high values of MRT and $T_{1/2}$ for PLGA-TMZ-NP TF-PLGA-TMZ-NP are indicative of slow clearance and long blood circulation of drug nanoparticles.

The distribution results show high accumulation of TMZS than PLGA-TMZ-NP and Tf-PLGA-TMZ-NP in liver. At 0.5hrs after injection, TMZS shows 60.65%A/g as compared to 44.92%A/g and 28.39%A/g for PLGA-TMZ-NP and Tf-PLGA-TMZ-NP respectively.

The low accumulation of nanoparticles may be due to the hydrophilicity associated with the nanoparticle surface, as mentioned earlier. Further, transferrin as reported could have masked the recognization sites on the colloidal systems thereby reducing the liver uptake [Litzinger et al., 1994; Soni V. et al., 2008]. The uptake of temozolomide in solution form was higher in spleen initially; however at 24hrs the radioactivity measured in spleen was higher for nanoparticles. The uptake of temozolomide was found to be higher in spleen with 13.33 %A/g at 0.5hrs compared to the 8.11%A/g and 8.25%A/g for unconjugated and conjugated nanoparticles. However, the nanoparticle accumulation was found to increase with time depicting PLGA-TMZ-NP and Tf-PLGA-TMZ-NP detection in spleen with 10.42%A/g and 12.01A%/g at 2hrs.

The distribution results in the kidney indicate higher values for TMZS then PLGA-TMZ-NP and Tf- PLGA-TMZ-NP. At 0.5hrs after intravenous injection, TMZS shows higher accumulation in kidney at 16.29%A/g with respect to 6.51%A/g for PLGA-TMZ-NP and 5.08%A/g for Tf- PLGA-TMZ-NP, indicating fast clearance of temozolomide solution than the nanoparticle formulation. The radioactivity at 24hrs is lower for TMZS (0.69%A/g) as that of PLGA-TMZ-NP (2.23%A/g) and Tf- PLGA-TMZ-NP (2.41%A/g), confirming the higher elimination half life for drug encapsulated PLGA nanoparticles.

The radioactivity measured indicates higher accumulation of unconjugated and conjugated nanoparticles than plain temozolomide in the lungs. This enhanced deposition is resulted due to the size of the nanoparticles.

The results depict higher accumulation of free drug in heart than the Temozolomide loaded unconjugated and conjugated nanoparticles, indicative of potential reduction in cardiotoxicity associated with temozolomide using the nanoparticle formulation.

Figure 9.5: Brain concentration Vs. Time (hr) plot for ^{99m}Tc Temozolomide formulations

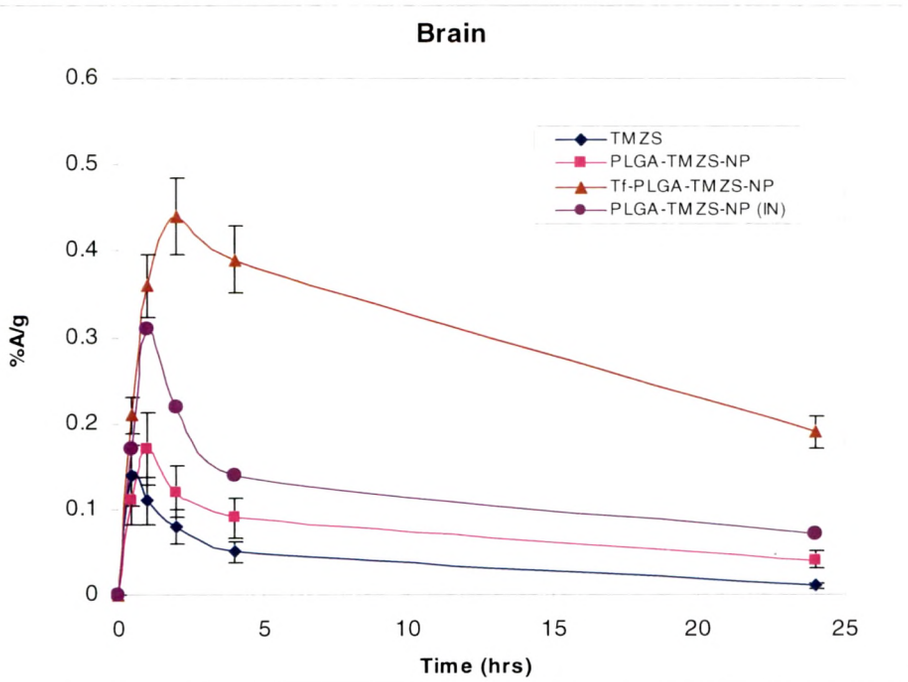

The brain distribution curve of TMZS, PLGA-TMZ-NP (IV), Tf-PLGA-TMZ-NP and PLGA-TMZ-NP (IN) is shown in Figure 9.5. It is evident from results that the brain uptake of temozolomide in solution form was lower than the nanoparticle formulations. The peak concentration for TMZS in brain was found to be 0.14%A/g at 0.5hrs after intravenous injection. At 24hrs, the concentration of TMZS in brain recorded was not detectable. The distribution of nanoparticle formulations demonstrate enhanced deposition in the brain. The peak concentrations for PLGA-TMZ-NP and Tf-PLGA-TMZ-NP were found to be 0.17%A/g and 0.44%A/g attained at 1hr and 2hrs respectively after intravenous administration. AT 24hrs after intravenous injection the unconjugated nanoparticles show 4 folds increase in brain concentration i.e. 0.04%A/g, as that of TMZS. Tf conjugated nanoparticles with 0.19%A/g at 24hrs, 4.75 folds higher uptake in brain than unconjugated nanoparticles. Also, the radioactivity observed after 24hrs for Tf-PLGA-TMZ was even higher than the peak concentration of TMZS.

The intranasal administration of PLGA-TMZ-NP led to significantly superior brain deposition than the intravenous injection of same formulation and plain drug solution. The brain concentrations at 0.5hr and 1hr post intranasal administration of PLGA-TMZ-NP were found to be 0.17%A/g and 0.31%A/g respectively. At 24hrs, the brain concentrations were 1.75times that of the same formulation administered intravenously. However, overall brain accumulation after intranasal administration of PLGA-TMZ-NP was significantly lower when compared with intravenous injection of Tf-PLGA-TMZ-NP.

Table 9.12: AUC values of brain for Temozolomide formulations

Parameter/ Formulation	TMZS	PLGA-TMZ-NP (IV)	TF- PLGA-TMZ-NP	PLGA-TMZ-NP (IN)
AUC (0→24) (hr)*(%A/g)	0.8161	1.4579***	6.9863*	2.7987**
AUC (0→∞) (hr)*(%A/g)	0.9287	1.9810***	12.0839*	4.3543**

* P<0.05, Significant difference with Tf-PLGA-TMZ-NP as compared to other groups
** P<0.05, Significant difference with PLGA-TMZ-NP(IN) as compared to TMZS and PLGA-TMZ- NP (IV) groups
***P<0.05, Significantly higher than TMZS

The overall brain uptake demonstrated by AUC $_{(0\rightarrow 24)}$ brain for different groups is tabulated in table 9.6. The AUC $_{(0\rightarrow 24)}$ brain for Tf-PLGA-TMZ-NP was calculated to be 8.56 folds and 4.79 folds significantly higher than TMZS and PLGA-TMZ-NP after intravenous administration. When compared with intranasal administration of PLGA-TMZ-NP, AUC $_{(0\rightarrow 24)}$ brain for Tf-PLGA-TMZ-NP was 2.50 folds higher. However, PLGA-TMZ-NP after intranasal administration exhibits significantly higher brain AUC $_{(0\rightarrow 24)}$ at 1.92 folds and 3.43 folds compared to PLGA-TMZ-NP and TMZS administered intravenously.

The unconjugated and Tf conjugated nanoparticles show improved brain uptake of drug. The hydrophilic surface characteristic of the nanoparticles is believed to have led to increase in the residence time in blood and thereby preventing early clearance of the drug from the body and availability for brain uptake. Tf conjugated nanoparticles show preferential accumulation in brain, due to receptor mediated endocytosis through the abundant transferrin receptors at the BBB. [Pardridge et al., 1987; Roberts et al., 1993; Mishra et al., 2006; Soni et al., 2008] Also, the actual condition of brain tumors leads to

disruption of BBB, which may further enhance the better accumulation of the delivery system [Ningaraj, 2006]. The intranasal administration of PLGA-TMZ-NP increased brain concentrations as compared to the intravenous administration of same formulation and TMZS. The lower blood concentration achieved after the intranasal administration of the unconjugated nanoparticles indicates the direct transport of the nanoparticles to the brain through the olfactory route bypassing the blood brain barrier.

Gamma Scintigraphy Studies

To ascertain the brain targeting following intravenous administration of ^{99m}TC temozolomide loaded nanoparticles, gamma scintigraphy was performed and scintigrams after 2 hrs post intravenous injection are shown in Figure 9.6.

Figure 9.6: Gamma Scintigraphy image of mice after 2hrs of intravenous injection of TMZS (A), PLGA-TMZ-NP (B) and Tf-PLGA-TMZ-NP (C)

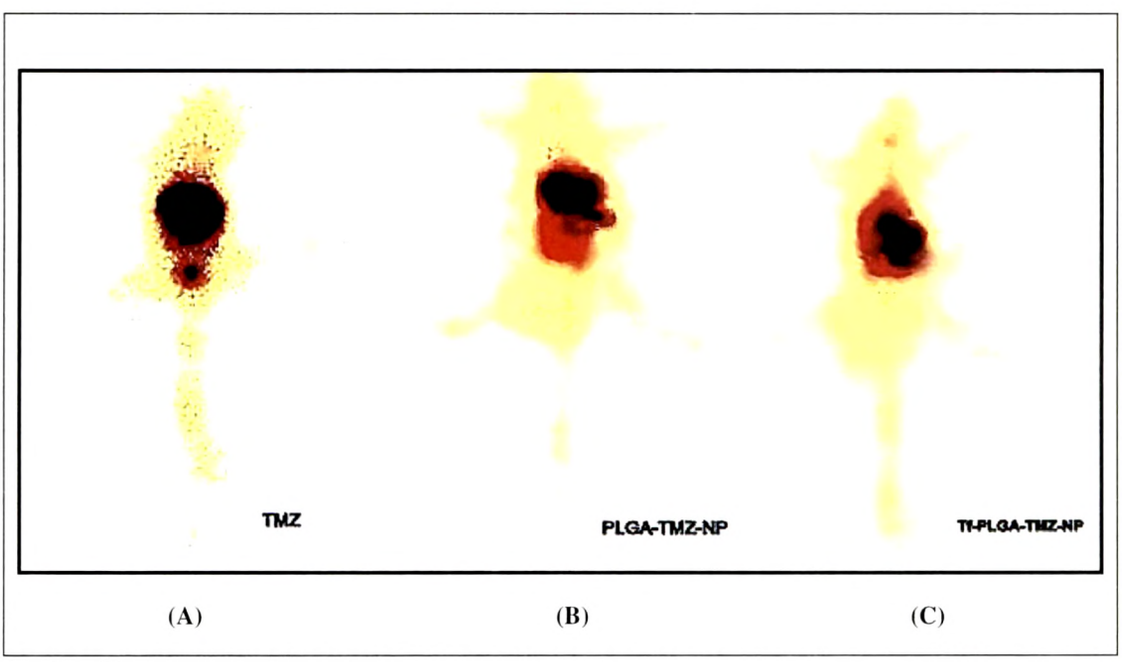

The major radioactivity deposition is seen in liver and spleen, in confirmation to the biodistribution studies. The brain deposition shows higher accumulation of Tf-PLGA-TMZ-NP in brain, following intravenous administration, as compared to PLGA-TMZ-NP and TMZS is clearly depicted in the scintigram.

9.3 Conclusions

To conclude, significant improvement in brain uptake was observed following intravenous administration of transferrin conjugated Etoposide/temozolomide nanoparticles compared to unconjugated nanoparticles and drug solution due to receptor mediated intracellular transcytosis through transferrin receptors present in the blood brain barrier coupled with intercellular transcytosis of the nanoparticles. The un- conjugated nanoparticles led higher brain uptake compared to drug solution and may be attributed to more lipophilic nature of PLGA nanoparticles having hydrophilic surface (PVA) for increasing blood circulation time. Brain uptake of nanoparticles may be due to predominant intercellular transcytosis. Similarly, the brain uptake of intranasally administered Etoposide/temozolomide loaded nanoparticles was also observed to be significantly higher compared to intravenously administered drug nanoparticles or drug solution but was significantly lower compared to transferrin conjugated drug nanoparticles. Faster and higher brain drug uptake after intranasal application may be due to direct nose to brain transport bypassing blood brain barrier. The transferrin conjugated drug nanoparticles were not assessed for brain uptake after intranasal administration due to scanty presence of transferrin receptor on human olfactory bulb in contrary to mice. The findings of this investigation suggest possible role of etoposide in treatment of brain tumours which is not a drug used in clinical practice for chemotherapy of brain tumours.

Temozolomide, currently used in therapy of brain tumours, is a prodrug and converts into its active metabolite for producing a therapeutic response. Temozolomide and its metabolite are reported to have short half life and hence require high dosing with increased dosing frequency. (www.fda.gov, Darkes et. al., 2002) The half life of the drug was observed to be enhanced by ~ 7.5folds and the brain deposition enhanced by ~ 8.56 folds. The prolonged release of temozolomide from the nanoparticles may lead to transport of Temozolomide in its intact form in brain and thereby making better availability of drug for conversion to active metabolite in brain, than the drug solution. Hence, it would be reasonable to anticipate that delivering the drug in nanoparticle form could lead to reduction in dose and dosing frequency.

References

- Abe, T., Hasegawa, S., Taniguchi, K., Yokomizo, A., Kuwano, T., Ono, M., Mori, T., Hori, S., Kohno, K., Kuwano, M., 1994. Possible involvement of multidrugresistance- associated protein (MRP) gene expression in spontaneous drug resistance to vincristine, etoposide and adriamycin in human glioma cells, Int. J. Cancer 58, 860–864.

- Akira, T., Ikumi, T., 1997. Blood brain barrier function of P-glycoprotein, Adv. Drug Deliv. Rev. 25, 287-298

- Angela, R.J., Eric, V.S, 2007. Blood-Brain Barrier Transport of Therapeutics via Receptor-Mediation, Pharmaceutical Research Vol. 24, No. 9, 1759-1771

- Begley, D.J., 1996. The blood–brain barrier: principles for targeting peptides and drugs to the central nervous system. J. Pharm. Pharmacol. 48,136–146

- Darkes et. al, 2002. Temozolomide: A Review of its Use in the Treatment of Malignant Gliomas, Malignant Melanoma and Other Advanced Cancers, Am J Cancer, 1 (1), 55-80

- Illum, L., 2000. Transport of drugs from the nasal cavity to the central nervous system. Eur. J. Pharm. Sci. 11, 1–18.

- Jefferies, W.A., Brandon, M.R., Hunt, S.V., Williams, A.F., Gatter, K.C., Mason, D.Y., 1984. Transferrin receptor on endothelium of brain capillaries, Nature 312, 162-164

- Koike, K., Abe, T., Hisano, T., Kubo, T., Wada, M., Kohno, K., Kuwano, T., 1996. Overexpression of multidrug resistance protein gene in human cancer cell lines selected for drug resistance to epipodophyllotoxins, Jpn. J. Cancer Res. 87, 765–772.

- Litzinger D.C., Buiting A.M., Van Rooijen N., Huang L. 1994. Effect of liposome size on the circulation time and intra organ distribution of amphipathic poly (ethylene glycol)-containing liposomes. Biochem. Biophys. Acta. 1190, 99–107.

- Mishra, V., Mahor, S., Rawat, A., Gupta, P., Dubey, P., Khatri, K., & Vyas, S.P., 2006. Targeted brain delivery of AZT via transferrin anchored pegylated albumin nanoparticles, Journal of Drug Targeting, January 14(1), 45–53

- Moghimi, S.M., Hedeman, H., Muir, I.S., Illum, L., Davis, S.S., 1993. An investigation of the filtration capacity and the fate of large filtered sterically-stabilized microspheres in rat spleen. Biochin. Biophys. Acta 1157, 233–240

- Moos, T. and Morgan, E. H. 2000. Transferrin and transferrin receptor function in brain barrier systems. Cell Mol Neurobiol 20 (1), 77-95

- Ningaraj, N, 2006. Drug delivery to brain tumours: challenges and progress, Expert Opin. Drug. Deliv. 3(4), 499-509

- Pardridge, W.M., 1999. Blood-brain barrier biology and methodology. J Neurovirol 5 (6), 556-569

- Pardridge, W.M., Eisinberg, J., Yang, J., 1987. Human blood–brain barrier transferrin receptor. Metabolism 36, 892–895.

- Roberts, R.L., Fine, R.E., Sandra, A., 1993. Receptor-mediated endocytosis of transferrin at the blood–brain barrier. J. Cell Sci. 104, 521–532

- Sahoo, S.K. and Labhasetwar, V., 2005. Enhanced Antiproliferative Activity of Transferrin-Conjugated Paclitaxel-Loaded Nanoparticles Is Mediated via Sustained Intracellular Drug Retention Molecular Pharmaceutics, Vol. 2, No. 5, 373-383

- Sahoo, S.K.; Panyam, J.; Prabha, S.; Labhasetwar, V. 2002. Residual polyvinyl alcohol associated with poly (D,L-lactide-co-glycolide) nanoparticles affects their physical properties and cellular uptake. J. Control. Rel. 82, 105-114.

- Schlossauer, B. and Steuer, H., Comparative anatomy,physiology and in vitro models of the blood-brain and blood-retina barrier. Curr. Med. Chem. 2, 175-186, 2002

- Terasaki, T., Hosoya, K., 1999. The blood–brain barrier efflux transporters as a detoxifying system for the brain, Adv. Drug Deliv. Rev. 36, 195–209.

- Soni, V., Kohli, D.V., Jain, S.K., 2008, Transferrin-conjugated liposomal system for improved delivery of 5-fluorouracil to brain, Journal of Drug Targeting, January 16(1), 73–78

- www.fda.gov (Temodar)